COMPUTATIONAL MECHANICS
WCCM VI in conjunction with APCOM'04, Sept. 5-10, 2004, Beijing, China

A Stable Method for Fluid-Structure Interaction Problems

A. Masud[1*], R. A. Khurram[1], M.V. Bhana[1]

[1] *Department of Civil and Material Engineering, University of Illinois at Chicago, (M/C 246), 842 W. Taylor St. Chicago, Illinois, 60607, USA.*
e-mail: amasud@uic.edu, kroohu1@uic.edu, mbhana1@uic.edu

Abstract This paper presents a stabilized finite element formulation for the incompressible Navier-Stokes equations, written in an arbitrary Lagrangian-Eulerian frame to model flow problems that involve moving and deforming meshes. The stabilized formulation is derived based on the varriational multiscale method proposed by Hughes [1], and employed in [2,3] to study advection dominated diffusion phenomena. A significant feature of the present method is that the definition of the stabilization terms appear naturally, and therefore the formulation is free of any user-defined parameters. A mesh moving technique is integrated in this formulation to accommodate the motion of the computational domain and to map the moving boundaries in a rational way. The method is tested on a periodic oscillating elastic beam in a fluid domain.

Key words: Multiscale methods, Arbitrary Lagrangian-Eulerian (ALE), Fluid-Structure-Interaction (FSI), Oscillating beam, Moving boundaries

INTRODUCTION

As CFD tools are becoming more popular and widespread in engineering analysis and design, there is a growing trend towards applying these methods to analyze and understand more complex problems. Fluid structure interaction (FSI) problems are classical examples of such involved multi-physics applications. FSI problems require stabilized mathematical formulations for the Navier-Stokes equations that are then written in an arbitrary Lagrangian-Eulerian (ALE) frame. The ALE descriptions are based on the notion of an arbitrary movement of the reference frame, which is continuously rezoned in order to allow a precise description of the moving interfaces. As such, ALE methods require mesh update techniques for the fluid mesh so that the same computational mesh with adaptive rezoning can be used for successive transient calculations. This rezoning is typically continued until the condition number of the elements in the deforming meshes starts deteriorating. At this point, a new mesh is usually constructed by freezing the calculations in time, and the information is transferred from the old mesh on to the new mesh using a projection algorithm.

It is well documented that the standard Galerkin formulations for the incompressible Navier-Stokes equations suffer from several numerical deficiencies. First, the convection term needs special attention, and second, the practically convenient combinations of various interpolation functions for the velocity and the pressure fields often do not work. The last two decades have seen great progress in the development of stabilized methods for the Navier-Stokes equations. The two most celebrated approaches are the Streamline Upwind/Petrov-Galerkin (SUPG) method [4], and the Galerkin/Least-Squares (GLS) method [5] (and references therein). In this paper we present a stabilized formulation for the incompressible Navier-Stokes equations that is derived based on the Variational Multiscale framework proposed by Hughes [1]. The present formulation inherits the stability properties of the celebrated stabilized methods, i.e., the SUPG and the GLS methods. The most notable feature of the present method is that the stabilization terms appear naturally in the derivation. The formulation is written in an ALE frame for application to FSI problems, and is integrated with an automatic mesh moving scheme that accounts for the moving and deforming fluid meshes.

An outline of the paper is as follow. We first present the strong and weak forms of the incompressible Navier-Stokes equations, expressed in the ALE form. Then we present the multiscale method. The mesh motion scheme which is an integral part of FSI solution strategy is presented next. Lastly, the numerical results for large amplitude oscillation of an elastic beam in the surrounding fluid domain are presented to show the superior properties of the method.

THE STRONG FROM

Let $\Omega \subset \Re^{n_{sd}}$ be an open bounded region with piecewise smooth boundary Γ. We assume $n_{sd} \geq 2$. The incompressible Navier-Stokes equations in arbitrary Eulerian-Lagrangian framework can be written as

$$\frac{\partial \mathbf{v}}{\partial t} + (\mathbf{v} - \mathbf{v}_m) \cdot \nabla \mathbf{v} - 2\nu \nabla \cdot \varepsilon(\mathbf{v}) + \nabla p = \mathbf{f} \qquad \text{in } \Omega \times [0,T] \tag{1}$$

$$\operatorname{div} \mathbf{v} = 0 \qquad \text{in } \Omega \times [0,T] \tag{2}$$

$$\mathbf{v} = \mathbf{g} \qquad \text{on } \Gamma_g \times [0,T] \tag{3}$$

$$\mathbf{n} \cdot (2\nu\varepsilon(\mathbf{v}) - p\mathbf{I}) = \mathbf{h} \qquad \text{on } \Gamma_h \times [0,T] \tag{4}$$

$$\mathbf{v}(\mathbf{x},0) = \mathbf{v}_0(\mathbf{x}) \qquad \mathbf{x} \in \Omega \tag{5}$$

where the functions $\mathbf{f} : \Omega \to \Re^{n_{sd}}$, $\mathbf{g} : \Gamma_g \to \Re^{n_{sd}}$ and $\mathbf{h} : \Gamma_h \to \Re^{n_{sd}}$ as well as the initial solenoidal velocity $\mathbf{v}_0 : \Omega \to \Re^{n_{sd}}$ are assumed given. The strain rate tensor is defined as

$$\varepsilon(\mathbf{v}) = \frac{1}{2}(\nabla \mathbf{v} + (\nabla \mathbf{v})^T) \tag{6}$$

and $\mathbf{I}$ is the identity tensor. $\mathbf{v}$ is the unknown flow velocity, $\mathbf{v}_m$ is the mesh velocity and p is the kinematic pressure i.e., pressure divided by density. Γ_g and Γ_h indicate the Dirichlet and Neumann parts of the boundary, respectively, with the usual conditions $\Gamma = \Gamma_g \cup \Gamma_h$ and $\Gamma_g \cap \Gamma_h = \emptyset$. The unit normal vector pointing outward is indicated as $\mathbf{n}$. The kinematic viscosity ν is assumed to be positive and constant throughout the domain.

1. The standard weak form

Find $\mathbf{v} \in \mathcal{U} = (H_0^1(\Omega))^{n_{sd}}$ and $p \in P = C^0(\Omega) \cap L^2(\Omega)$ such that

$$(\mathbf{w}, \frac{\partial \mathbf{v}}{\partial t})_\Omega + (\mathbf{w}, (\mathbf{v} - \mathbf{v}_m) \cdot \nabla \mathbf{v})_\Omega + (\nabla \mathbf{w}, \nu \nabla \mathbf{v})_\Omega - (\nabla \cdot \mathbf{w}, p)_\Omega + (q, \nabla \cdot \mathbf{v})_\Omega = (\mathbf{w}, \mathbf{f})_\Omega + (\mathbf{w}, \mathbf{h})_{\Gamma_h} \quad \forall \{\mathbf{w}, p\} \in \mathcal{U} \times P \tag{7}$$

THE VARIATIONAL MULTISCALE METHOD

1. Multiscale decomposition

In this section we present the Hughes' Variational Multiscale (HVM) approach [1]. We consider the bounded domain Ω discretized into non-overlapping regions Ω^e (element domains) with boundaries Γ^e, e =1, 2…….n_{umel} such that

$$\Omega = \bigcup_{e=1}^{n_{umel}} \overline{\Omega^e} \tag{8}$$

We denote the union of element interiors and element boundaries by Ω' and Γ', respectively.

$$\Omega' = \bigcup_{e=1}^{n_{umel}} (\text{int})\,\Omega^e \quad \text{(element interiors)} \tag{9}$$

$$\Gamma' = \bigcup_{e=1}^{n_{umel}} \Gamma^e \qquad \text{(element boundaries)} \tag{10}$$

We assume an overlapping sum decomposition of the velocity field into coarse scales or resolvable scales and fine scales or the subgrid scales. Fine scales can be viewed as components associated with the regions of high velocity gradients.

$$\mathbf{v}(\mathbf{x}) = \bar{\mathbf{v}}(\mathbf{x}) + \mathbf{v}'(\mathbf{x}) \tag{11}$$

$$\mathbf{w}(\mathbf{x}) = \bar{\mathbf{w}}(\mathbf{x}) + \mathbf{w}'(\mathbf{x}) \tag{12}$$

We further make an assumption that the subgrid scales although non-zero within the elements, vanish identically over the element boundaries.

$$\mathbf{u}' = \mathbf{w}' = 0 \qquad \text{on} \quad \Gamma' \tag{13}$$

We now introduce the appropriate spaces of functions for the coarse and fine scale fields and specify direct sum decomposition on these spaces.

$$\mathcal{U} = \bar{\mathcal{U}} \oplus \mathcal{U}' \tag{14}$$

where $\mathcal{U}$ in (14) is the space of trial solutions and weighting functions for the coarse scale velocity field and is identified with the standard finite element space. On the other hand, various characterizations of $\mathcal{U}'$ are possible, subject to the restriction imposed by the stability of the formulation that requires $\bar{\mathcal{U}}$ and $\mathcal{U}'$ to be linearly independent. Consequently, in the discrete case $\mathcal{U}'$ can contain various finite dimensional approximations, e.g., bubble functions or p-refinements, which satisfy (13). Likewise the pressure field can be assumed to be decomposed into coarse and fine scales. Without loss of generality we assume that fine scale pressure field is zero.

2. The variational multiscale problem

The linearized convection term can be written as

$$(\mathbf{w}, \mathbf{v}_c \cdot \nabla \mathbf{v})_\Omega \tag{15}$$

where $\mathbf{v}_c$ is the converged velocity from previous step. Employing (15) in (7), and then substituting the trial solutions (11) and the weighting functions (12) in (7) we get the following form

$$\begin{aligned}&(\bar{\mathbf{w}} + \mathbf{w}', \frac{\partial \bar{\mathbf{v}}}{\partial t})_\Omega + (\bar{\mathbf{w}} + \mathbf{w}', (\mathbf{v}_c - \mathbf{v}_m) \cdot \nabla(\bar{\mathbf{v}} + \mathbf{v}'))_\Omega + (\nabla(\bar{\mathbf{w}} + \mathbf{w}'), \nu \nabla(\bar{\mathbf{v}} + \mathbf{v}'))_\Omega \\ &- (\nabla \cdot (\bar{\mathbf{w}} + \mathbf{w}'), p)_\Omega + (q, \nabla \cdot (\bar{\mathbf{v}} + \mathbf{v}'))_\Omega = (\bar{\mathbf{w}} + \mathbf{w}', \mathbf{f})_\Omega + (\bar{\mathbf{w}} + \mathbf{w}', \mathbf{h})_{\Gamma_h}\end{aligned} \tag{16}$$

With suitable assumptions on the fine scale field, as stipulated in (13), and employing the linearity of the weighting function slot, we can split the problem into the coarse and the fine scale parts, indicated as $\bar{\mathcal{W}}$ and $\mathcal{W}'$, respectively.

The coarse scale problem $\bar{\mathcal{W}}$

$$\begin{aligned}&(\bar{\mathbf{w}}, \frac{\partial \bar{\mathbf{v}}}{\partial t})_\Omega + (\bar{\mathbf{w}}, (\mathbf{v}_c - \mathbf{v}_m) \cdot \nabla(\bar{\mathbf{v}} + \mathbf{v}'))_\Omega + (\nabla \bar{\mathbf{w}}, \nu \nabla(\bar{\mathbf{v}} + \mathbf{v}'))_\Omega - (\nabla \cdot \bar{\mathbf{w}}, p)_\Omega + (q, \nabla \cdot (\bar{\mathbf{v}} + \mathbf{v}'))_\Omega \\ &= (\bar{\mathbf{w}}, \mathbf{f})_\Omega + (\bar{\mathbf{w}}, \mathbf{h})_{\Gamma_h}\end{aligned} \tag{17}$$

The fine scale problem $\mathcal{W}'$

$$(\mathbf{w}', \frac{\partial \bar{\mathbf{v}}}{\partial t})_{\Omega'} + (\mathbf{w}', (\mathbf{v}_c - \mathbf{v}_m) \cdot \nabla(\bar{\mathbf{v}} + \mathbf{v}'))_{\Omega'} + (\nabla \mathbf{w}', \nu \nabla(\bar{\mathbf{v}} + \mathbf{v}'))_{\Omega'} - (\nabla \cdot \mathbf{w}', p)_{\Omega'} = (\mathbf{w}', \mathbf{f})_{\Omega'} \tag{18}$$

3. Solution of the fine scale problem (W')

Exploiting linearity of the solution slot in (18) we have

$$(\mathbf{w}', \frac{\partial \bar{\mathbf{v}}}{\partial t})_{\Omega'} + (\mathbf{w}', (\mathbf{v}_c - \mathbf{v}_m) \cdot \nabla \bar{\mathbf{v}})_{\Omega'} + (\mathbf{w}', (\mathbf{v}_c - \mathbf{v}_m) \cdot \nabla \mathbf{v}')_{\Omega'} + (\nabla \mathbf{w}', \nu \nabla \bar{\mathbf{v}})_{\Omega'} + (\nabla \mathbf{w}', \nu \nabla \mathbf{v}')_{\Omega'} - (\nabla \cdot \mathbf{w}', p)_{\Omega'} = (\mathbf{w}', \mathbf{f})_{\Omega'} \tag{19}$$

Applying integration-by-parts to third and fifth terms on the left hand side of (19), we get

$$(\mathbf{w}', (\mathbf{v}_c - \mathbf{v}_m) \cdot \nabla \mathbf{v}')_{\Omega'} + (\nabla \mathbf{w}', \nu \nabla \mathbf{v}')_{\Omega'} = (\mathbf{w}', \mathbf{f} - (\frac{\partial \bar{\mathbf{v}}}{\partial t} + (\mathbf{v}_c - \mathbf{v}_m) \cdot \nabla \bar{\mathbf{v}} - \nu \nabla^2 \bar{\mathbf{v}} + \nabla p)_{\Omega'} \tag{20}$$

To crystallize the ideas, and without loss of generality, we assume that the fine scales are represented via bubbles over element domains, i.e.,

$$\mathbf{v}'|_{\Omega'} = b_1^e \mathbf{v}'_e \tag{21}$$

$$\mathbf{w}'|_{\Omega'} = b_2^e \mathbf{w}'_e \tag{22}$$

where b_1^e and b_2^e represent the bubble shape functions for the fine scale trial solutions and the fine scale weighting functions, respectively. For details, consult [3]. Furthermore, $\mathbf{v}'_e$ and $\mathbf{w}'_e$ represent the coefficients for the fine scale trial solutions and the weighting functions, respectively. Substituting (21) and (22) in the fine scale problem (20) we get

$$\mathbf{v}'(\mathbf{x}) = -\tau \, (\frac{\partial \bar{\mathbf{v}}}{\partial t} + (\mathbf{v}_c - \mathbf{v}_m) \cdot \nabla \bar{\mathbf{v}} - \nu \nabla^2 \bar{\mathbf{v}} + \nabla p - \mathbf{f}) \tag{23}$$

where

$$\tau = b_1^e \int_{\Omega'} b_2^e d\Omega \left[\int_{\Omega'} b_2^e (\mathbf{v}_c - \mathbf{v}_m) \cdot \nabla b_1^e d\Omega \mathbf{I} + \nu \int_{\Omega'} |\nabla b_2^e \| \nabla b_1^e| d\Omega \mathbf{I} + \nu \int_{\Omega'} \nabla b_2^e \otimes \nabla b_1^e d\Omega \right]^{-1} \tag{24}$$

4. The coarse scale problem ($\bar{W}$)

Exploiting linearity of the solution slot in (17) we have

$$(\bar{\mathbf{w}}, \frac{\partial \bar{\mathbf{v}}}{\partial t})_{\Omega} + (\bar{\mathbf{w}}, (\mathbf{v}_c - \mathbf{v}_m) \cdot \nabla \bar{\mathbf{v}})_{\Omega} + (\bar{\mathbf{w}}, (\mathbf{v}_c - \mathbf{v}_m) \cdot \nabla \mathbf{v}')_{\Omega} + (\nabla \bar{\mathbf{w}}, \nu \nabla \bar{\mathbf{v}})_{\Omega} + (\nabla \bar{\mathbf{w}}, \nu \nabla \mathbf{v}')_{\Omega} - (\nabla \cdot \bar{\mathbf{w}}, p)_{\Omega} + (q, \nabla \cdot \bar{\mathbf{v}})_{\Omega} + (q, \nabla \cdot \mathbf{v}')_{\Omega} = (\bar{\mathbf{w}}, \mathbf{f})_{\Omega} + (\bar{\mathbf{w}}, \mathbf{h})_{\Gamma_h} \tag{25}$$

After integration-by-parts of third, fifth and ninth terms on left hand side of (25) and substituting fine scale solution from (23) into (25) we get

$$(\bar{\mathbf{w}}, \frac{\partial \bar{\mathbf{v}}}{\partial t})_{\Omega} + (\bar{\mathbf{w}}, (\mathbf{v}_c - \mathbf{v}_m) \cdot \nabla \bar{\mathbf{v}})_{\Omega} + (\nabla \bar{\mathbf{w}}, \nu \nabla \bar{\mathbf{v}})_{\Omega} - (\nabla \cdot \bar{\mathbf{w}}, p)_{\Omega} + (q, \nabla \cdot \bar{\mathbf{v}})_{\Omega} + ((((\mathbf{v}_c - \mathbf{v}_m) \cdot \nabla \bar{\mathbf{w}} + \nu \nabla^2 \bar{\mathbf{w}} + \nabla q), \tau (\frac{\partial \bar{\mathbf{v}}}{\partial t} + (\mathbf{v}_c - \mathbf{v}_m) \cdot \nabla \bar{\mathbf{v}} - \nu \nabla^2 \bar{\mathbf{v}} + \nabla p))_{\Omega} = (\bar{\mathbf{w}}, \mathbf{f})_{\Omega} + (\bar{\mathbf{w}}, \mathbf{h})_{\Gamma_h} + (((\mathbf{v}_c - \mathbf{v}_m) \cdot \nabla \bar{\mathbf{w}} + \nu \nabla^2 \bar{\mathbf{w}} + \nabla q), \tau \mathbf{f})_{\Omega} \tag{26}$$

5. The variational multiscale form

The stabilized form (26) is completely expressed in terms of the coarse/resolvable scales in the problem. Therefore, in order to keep the notation simple we drop the superposed bars and write the resulting form as

$$(\mathbf{w},\frac{\partial \mathbf{v}}{\partial t})_\Omega + (\mathbf{w},(\mathbf{v}_c - \mathbf{v}_m)\cdot\nabla\mathbf{v})_\Omega + (\nabla\mathbf{w},\nu\nabla\mathbf{v})_\Omega - (\nabla\cdot\mathbf{w},p)_\Omega + (q,\nabla\cdot\mathbf{v})_\Omega$$
$$+((((\mathbf{v}_c - \mathbf{v}_m)\cdot\nabla\mathbf{w} + \nu\nabla^2\mathbf{w} + \nabla q),\tau(\frac{\partial \mathbf{v}}{\partial t} + (\mathbf{v} - \mathbf{v}_m)\cdot\nabla\mathbf{v} - \nu\nabla^2\mathbf{v} + \nabla p))_\Omega \qquad (27)$$
$$= (\mathbf{w},\mathbf{f})_\Omega + (\mathbf{w},\mathbf{h})_{\Gamma_h} + (((\mathbf{v}_c - \mathbf{v}_m)\cdot\nabla\mathbf{w} + \nu\nabla^2\mathbf{w} + \nabla q),\tau\mathbf{f})_\Omega$$

MESH MOVING SCHEME

A major challenge in the fluid-structure interaction problems lies in the development of a mesh rezoning technique to adapt the fluid mesh to the changing spatial domain. In this section we have implemented a mesh motion technique (proposed in [6]) which is appropriate for arbitrarily shaped domains. The formal statement of the boundary-value problem can be written as:

Given **g**, the prescribed displacements at the moving boundary, find the mesh displacement field $\mathbf{u}:\Omega\rightarrow\Re^{n_{sd}}$, such that

$$\nabla\cdot(1+\tau_m)\nabla\mathbf{u} = 0 \qquad \text{in } \Omega \qquad (28)$$

$$\mathbf{u} = \mathbf{g} \qquad \text{on } \Gamma_m \qquad (29)$$

$$\mathbf{u} = \mathbf{0} \qquad \text{on } \Gamma_f \qquad (30)$$

where Γ_m and Γ_f indicate the moving and fixed parts of the boundary, respectively. τ_m is a bounded, non-dimensional function which is designed to prevent the inversion of small elements in the high resolution regions of the fluid mesh. A simple definition of τ_m is given in [6].

This mesh moving scheme is then applied to an oscillating beam. Figure 1 shows the initial mesh, consisting of 24,068 3-node elements. The mesh has high resolution around the beam to capture the physics in the boundary layer region. Figure. 2 shows the zoomed view of the deformed mesh. The smaller elements close to the moving interfaces translate with the least amount of distortion, and the larger elements in the far field deform more to absorb the motion. Consequently, the shape of the elements is maintained in the boundary layer regions, resulting in a well-defined mesh.

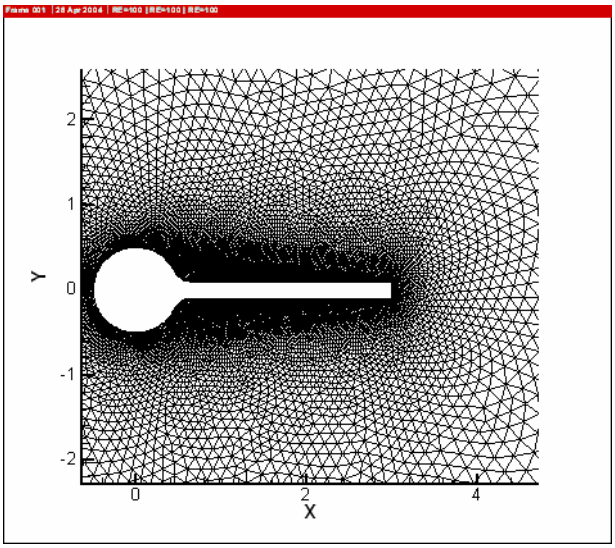

Fig. 1 Initial zoomed mesh

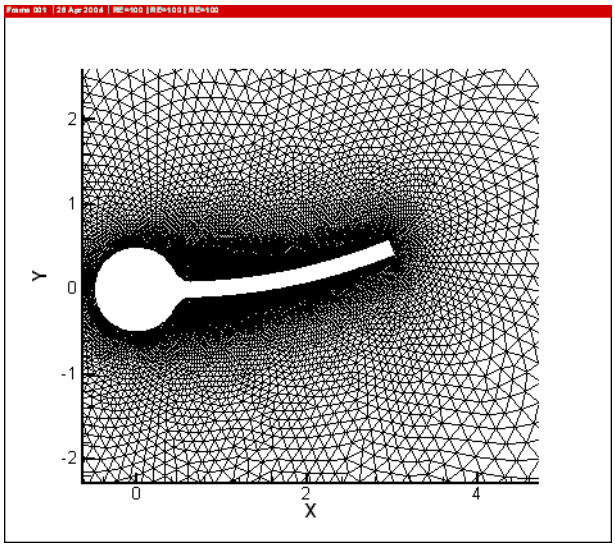

Fig. 2 Deformed zoomed mesh

NUMERICAL RESULTS

1. Oscillating elastic beam in fluid domain

Figure 3 shows the schematics of the problem. Inflow conditions are imposed at the left boundary, while free stream conditions are assumed at the top and bottom boundary. Exit (zero stress) condition is assumed at the right boundary. Reynolds number is 100.

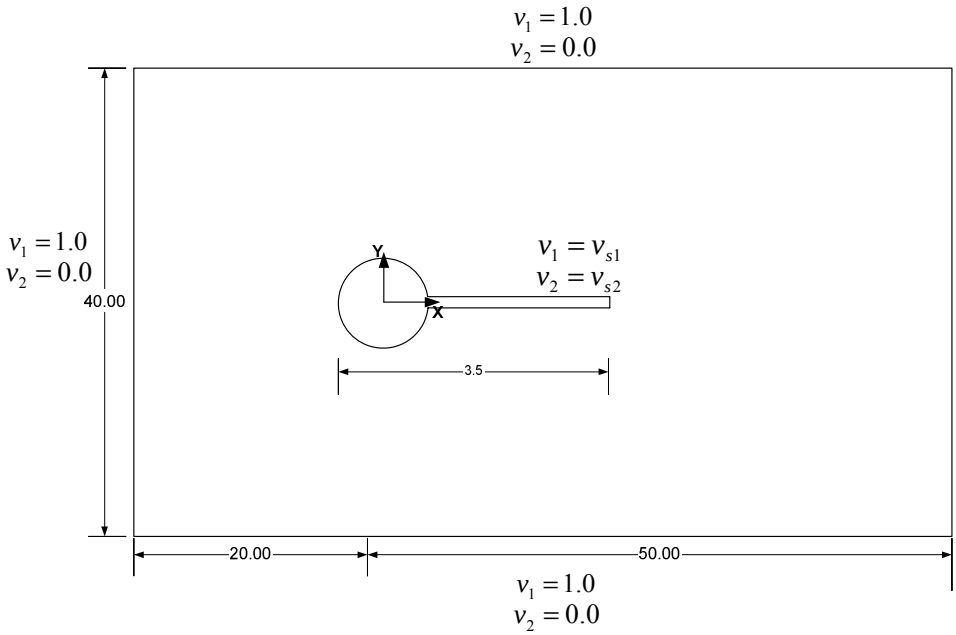

Fig. 3 Schematics of the elastic beam vibrating in fluid domain

The beam is given a prescribed periodic oscillation. The beam is kept stationary for the first 100 time steps. In the next 50 time steps, the beam moves upwards in a prescribed motion and attains maximum amplitude. In the next 50 time steps the beam comes back to the mean position and then it follows downward. The complete cycle is done in 200 time steps. In order to get the idea of the magnitudes of mesh velocity as compared with the free stream velocity, the velocity of the node at the tip of the beam is plotted in Fig. 4. Also shown is the mean velocity of the flow field.

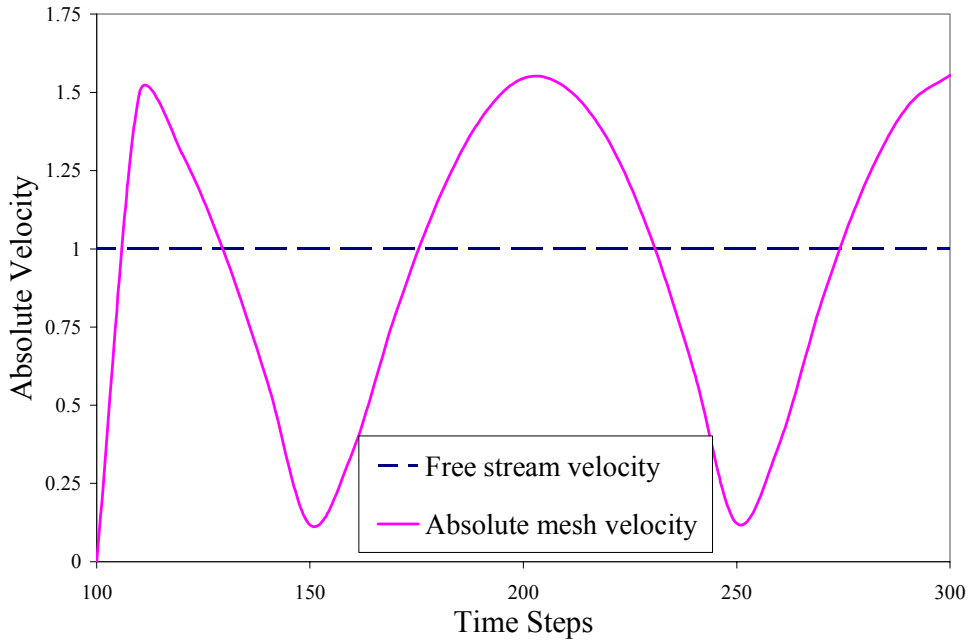

Fig. 4 Comparison of the free stream velocity with the mesh velocity (at the tip of the beam)

The mesh velocity dominates the flow field at various instants. Figure 5 shows the dimensionless pressure coefficient C_p in the upward motion, i.e., from 100 – 150 time steps. High pressure region can be seen on the top surface of the beam and the suction effects can be seen at the bottom surface. This situation reverses in Fig. 6 which shows the C_p in the downward motion i.e. 150 – 200 time steps. Fig. 7 shows the C_p line plots on the upper surface of the beam, at various time steps. Although the separation effect in the wake of the round body and at the edge of beam is visible, at the 100th time step the C_p is almost zero throughout length of the beam. At the 110th time step, as the beam starts moving up, the pressure increases instantaneously. The high pressure at the upper surface is maintained until the beam reaches its highest amplitude. Then the suction effects are visible from time steps 150 – 200. The pressure profile shows the wake effect of the cylindrical body and the edge effects of the beam.

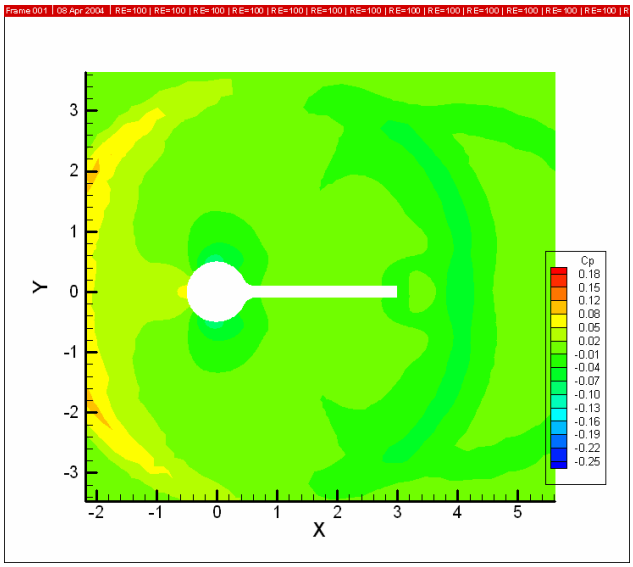

100 time steps

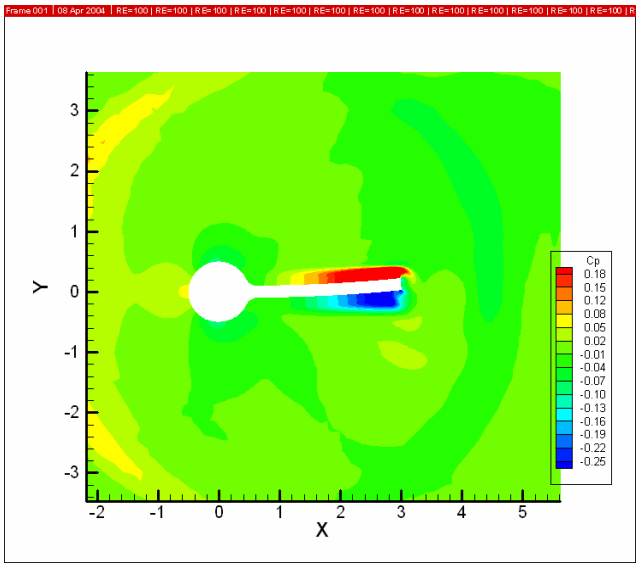

110 time steps

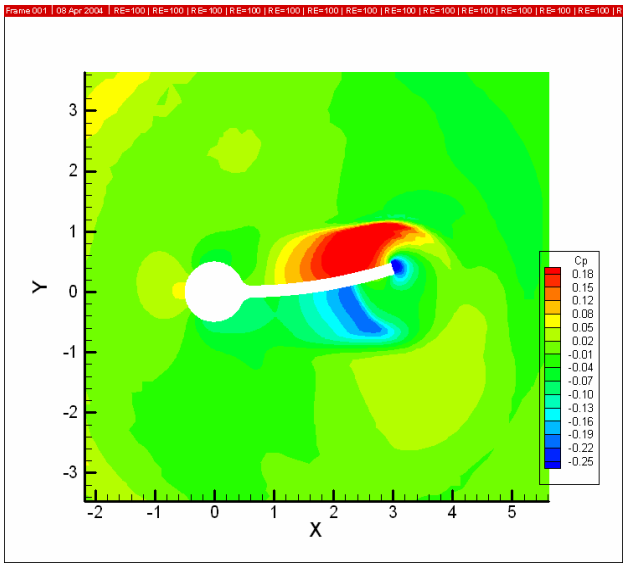

130 time steps

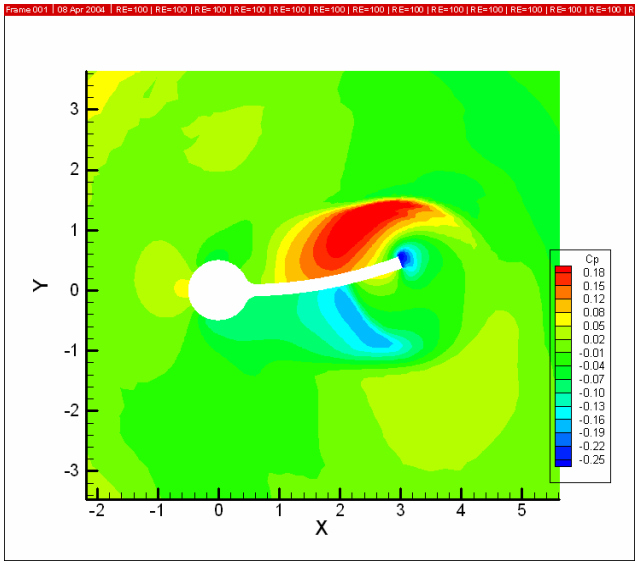

140 time steps

Fig. 5 C_p contours at various instances during the upward motion of the beam

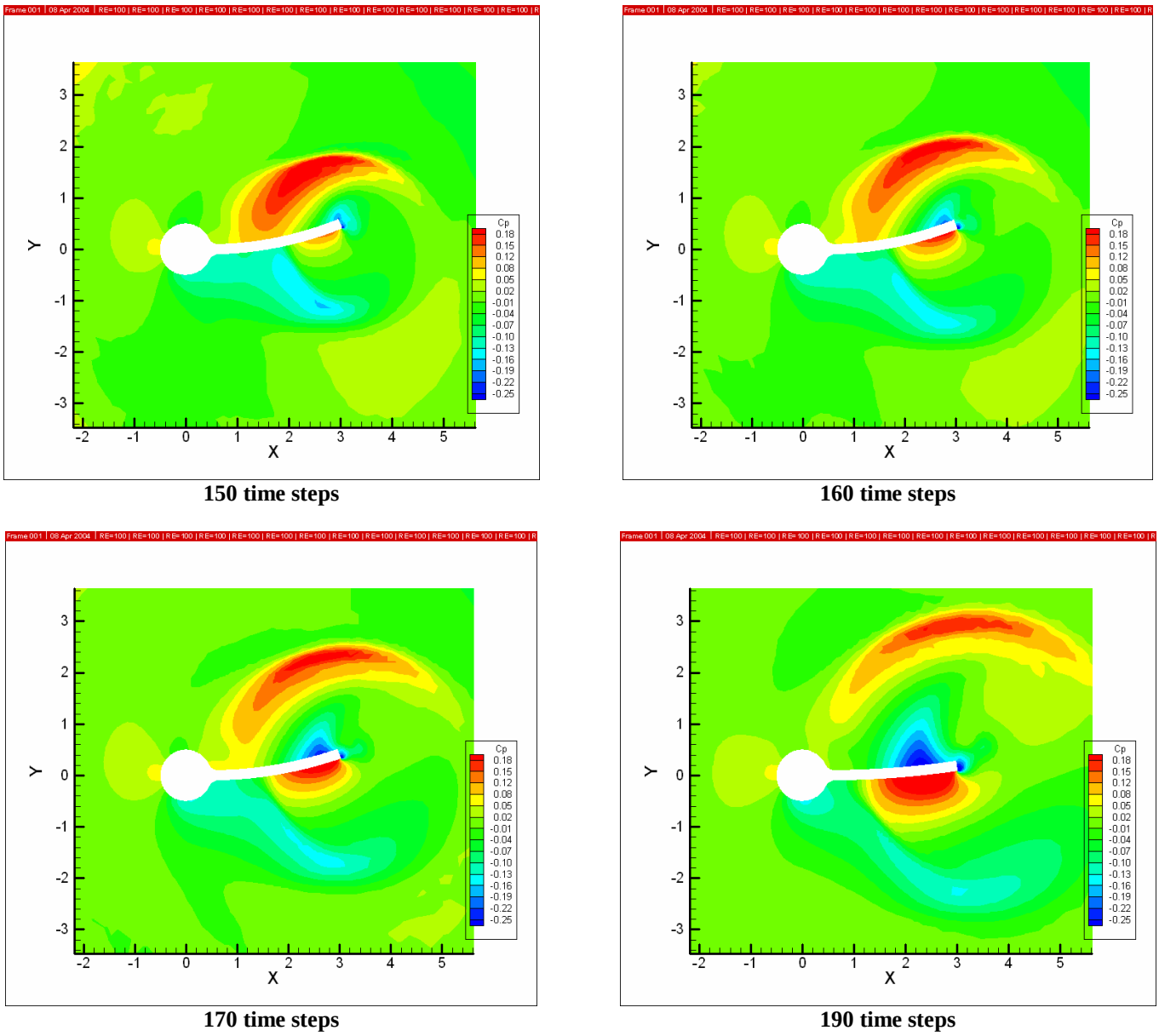

Fig. 6 C_p contours at various instances during the downward motion of the beam

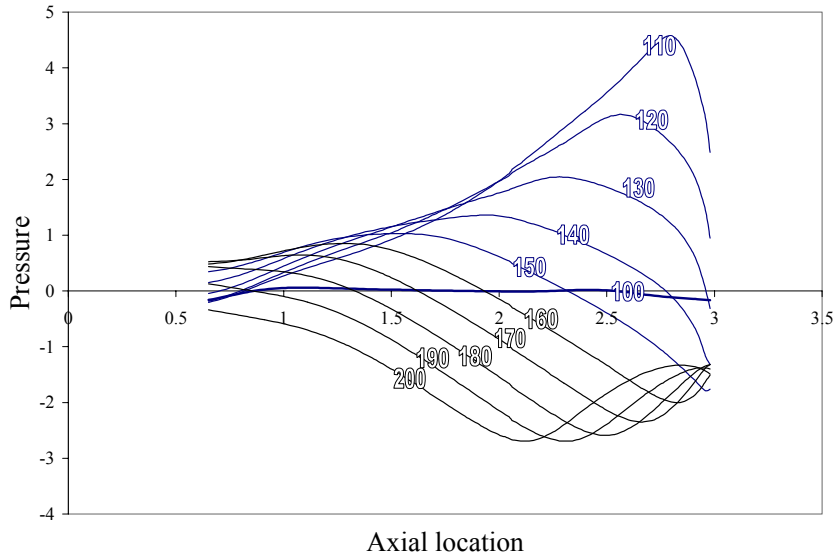

Fig. 7 Line plots of C_p at the upper surface of the beam at various time steps

CONCLUSIONS

We have presented a stabilized formulation for the incompressible Navier-Stokes equations on moving grids. In this formulation the stabilization terms appear naturally as a result of the decomposition of the velocity field into the coarse and the fine scales. The proposed method exhibits the superior stability properties of the SUPG and the GLS methods. An important feature of the formulation is that, unlike the SUPG and the GLS methods, a definition of the stability parameter "τ" appears naturally in the derivation. The method is applied to FSI problems that require mesh rezoning techniques to update the fluid mesh. In the mesh moving technique employed herein, the smaller elements translate together with the moving fluid-solid interfaces with the least amount of distortion while the larger elements that are away from the moving boundaries absorb most of the deformation. The stabilized/multiscale method integrated with mesh motion scheme is tested on a FSI problem involving large amplitude oscillation of an elastic beam in the fluid domain. Transient pressure contours are presented and line plots of the pressure profile on the surface of the beam are plotted. Numerical results show the good stability properties of the proposed method for this class of problems

Acknowledgements The support for this work was provided by the ONR grant N00014-02-1-0143. This support is gratefully acknowledged.

REFERENCES

[1] T.J.R. Hughes, Multiscale phenomena: *Green's functions, the Dirichlet-to-Neumann formulations, subgrid scale models, bubbles and the origins of stabilized methods*, Comput. Methods Appl. Mech. Engrg., 127, (1995), 387-401.

[2] A. Masud, *On a stabilized finite element formulation for incompressible Navier–Stokes equations, Proc. 4th US-Japan Conf., Tokyo, 2002*. CFD, Tokyo (2002).

[3] A. Masud, R.A. Khurram, *A multiscale/stabilized finite element method for the advection diffusion equation*, Comput. Methods Appl. Mech. Engrg., 193, (2004), 1997-2018.

[4] A.N.Brooks, T.J.R. Hughes, *Streamline upwind/Petrov –Galerkin formulations for convection dominated flows with particular emphasis on the incompressible Navier–Stokes equations*, Comput. Methods Appl. Mech. Engrg., 32, (1982), 199-259.

[5] T.J.R.Hughes, L.P.Franca, G.M.Hulbert, *A new finite element formulation for computational fluid dynamics: VIII. The Galerkin/least-squares method for advective –diffusive equations*, Comput. Methods Appl. Mech. Engrg., 73, (1989), 173-189.

[6] A. Masud, T.J.R.Hughes, *A space-time Galerkin/least-squares finite element formulation of the Navier-Stokes equations for moving domain problems*, Comput. Methods Appl. Mech. Engrg., 146, (1997), 91-126.

[7] Volker Gravemeier , Wolfgang A. Wall, Ekkehard Ramm, *A three level finite element method for the instationary incompressible Navier-Stokes equations*, Comput. Methods Appl. Mech. Engrg., 193, (2004), 1323-1366.

[8] Leopoldo P. Franca, A. Nesliturk, *On a two-level finite element method for the incompressible Navier-Stokes equations*, Int. J. Num. Meth. Eng, 52, (2001), 433-453.

[9] Leopoldo P.Franca, Sergio L. Frey, *Stabilized finite element methods: II. The incompressible Navier-Stokes equations,* Comput. Methods Appl. Mech. Engrg., 99, (1992), 209-233.

[10] T.E. Tezduyar, S. Mittal, S.E. Ray, R. Shih, *Incompressible flow computations with stabilized bilinear and linear equal-order-interpolation velocity-pressure elements*, Comput. Methods Appl. Mech. Engrg., 95, (1992), 221-242.

[11] Michel Lesoinne, Marcus Sarkis, Ulrich Hetmaniuk, Charbel Farhat, *A linearized method for the frequency analysis of three-dimensional fluid/structure interaction problems in all flow regimes*, Comput. Methods Appl. Mech. Engrg., 190, (2001), 3121-3146.

[12] Charbel Farhat, Philippe Geuzaine, Celine Grandmont, *The Discrete Geometric Conservation Law and the nonlinear stability of ALE schemes for the solution of flow problems on moving grid,* J. comput. Phy., 174, (2001), 669-694

[13] Philippe Geuzaine, Celine Grandmont, Charbel Farhat, *Design and analysis of ALE schemes with provable second-order time-accuracy for inviscid and viscous flow simulations,* J. Comput. Phy., 191, (2003), 206-227

[14] Bruno Koobus ,Charbel Farhat, *A variational multiscale method for the large eddy simulation of compressible turbulent flows on unstructured meshes—application to vortex shedding*, Comput. Methods Appl. Mech. Engrg., 193, (2004), 1367-1383